5826 *Chem. Mater.* **2009,** *21,* 5826–5835
DOI:10.1021/cm902741c

CHEMISTRY OF MATERIALS
Article

Proposed General Sol−Gel Method to Prepare Multimetallic Layered Double Hydroxides: Synthesis, Characterization, and Envisaged Application

Julia Prince,[†] Ascencion Montoya,[‡] Gerardo Ferrat,[‡] and Jaime S. Valente*[,†,‡]

[†]*Universidad Autonoma Metropolitana-A, Quimica de Materiales, Avenida San Pablo No. 180, 02200, Mexico, DF Mexico, and* [‡]*Instituto Mexicano del Petroleo, Eje Central No. 152, 07730, Mexico, DF Mexico*

Received September 2, 2009. Revised Manuscript Received October 26, 2009

A versatile sol−gel method for the synthesis of multimetallic layered double hydroxides (LDHs) is presented. The success of this method is due to the accurate control over crucial synthesis parameters, which are thoroughly analyzed, and to the complexation of metallic precursors in order to equalize their hydrolysis and condensation rates to obtain transparent gels. XRD patterns show pure LDH phase, with broad peaks indicative of small crystal size. Solids thus obtained show nanocapsular morphology, instead of the platelet-like particles obtained by coprecipitation and other methods. Thermal decomposition was analyzed by TGA, DTA, and FTIR, revealing that a variety of interlayer anions are present in different proportions, mainly carbonates, nitrates, acetates, and alkoxy groups. This observation was corroborated by the expansion in the interlayer region observed by XRD. N_2 physisorption confirmed that all calcined sol−gel LDHs have high specific surface areas (up to 290 $m^2\ g^{-1}$) and very narrow pore size distributions (ca. 3−4 nm). The sols are successfully cast as thin films over glass substrates; control over film thickness is achieved by varying aging time. Furthermore, catalytic membranes deposited over cordierite monoliths were obtained by immersion on sols and subsequent calcination; these membranes are chemically uniform, thermally stable, and well-adhered.

1. Introduction

Layered double hydroxides (LDHs), also known as hydrotalcite-like compounds or anionic clays, have received much attention in the past decades due to their vast applicability. An LDH is created when a fraction of the divalent cations in a brucite-like lattice are isomorphously replaced by trivalent cations, introducing a positive charge in the layers. This charge is electrically balanced by anions located in the interlayer region, along with hydration water molecules. Given the wide range of compounds with LDH structure that may be prepared, they are represented by the general formula: $[M^{II}_{(1-x)}M^{III}_{x}(OH)_2]A^{n-}_{x/n}\cdot mH_2O$, where M^{II} includes: Mg^{2+}, Co^{2+}, Cu^{2+}, Ni^{2+}, Zn^{2+}, etc.; M^{III} may be Al^{3+}, Cr^{3+}, Ga^{3+}, Fe^{3+}, etc.; and A^{n-} might be any organic and/or inorganic anion. Many ternary LDHs involving mixtures of different M^{II} and/or M^{III} may also be prepared.[1−3]

LDHs, and the mixed oxides obtained after their thermal decomposition, have been successfully employed as basic catalysts in numerous chemical reactions.[4−6] Furthermore, LDHs have several scientific and technological applications, such as hybrid composites, antacids, flame retardants, and PVC additives.[3] Several research groups worldwide have focused their attention in the intercalation of biological species and organic compounds between the layers in order to use LDHs in diverse fields as drug delivery carriers, sensing devices, etc.[3,7−9]

Traditionally, LDHs are synthesized by the coprecipitation of metallic salts with a concentrated alkaline solution. Several alternative methods have been proposed, depending on the intended application. For instance, an environmentally friendly method has been developed for industrial-scale production of multimetallic LDHs.[10] Also, control over the structural and textural properties of the final products has been recently attempted by procedures such as microwave irradiation,[11−13] ultrasonication,[11] or the urea hydrolysis method.[12,13] Another

*Corresponding author. Phone: +52 (55) 9175-8444. E-mail: jsanchez@imp.mx.

(1) Cavani, F.; Trifiro, F.; Vaccari, A. *Catal. Today* **1991**, *11*, 173.
(2) Rives, V. *Layered Double Hydroxides: Present and Future*; Nova Science Publishers: New York, 2001.
(3) Duan, X.; Evans, D. G. *Layered Double Hydroxides*; Structure and Bonding; Springer-Verlag: Berlin, 2006; Vol. *119*.
(4) Figueras, F. *Top. Catal.* **2004**, *29*, 189.
(5) Kumbhar, P. S.; Sanchez-Valente, J.; Figueras, F. *Chem. Commun.* **1998**, 1091.
(6) Figueras, F.; Lopez, J.; Sanchez-Valente, J.; Vu, T. T. H.; Clacencs, J. M.; Palomeque, J. *J. Catal.* **2002**, *211*, 144.
(7) Desigaux, L.; Belkacem, M. B.; Richard, P.; Cellier, J.; Léone, P.; Cario, L.; Leroux, F.; Taviot-Guého, C.; Pitard, B. Nano Lett. **2006**, Vol.*6*, No.2, 199.
(8) Yang, J. H.; Han, Y.-S.; Park, M.; Park, T.; Hwang, S.-J.; Choy, J.-H. *Chem. Mater.* **2007**, *19*, 2679.
(9) Khan, A. I.; O'Hare, D. *J. Mater. Chem.* **2002**, *12*, 3191.
(10) Valente, J. S.; Cantu, M. S.; Figueras, F. *Chem. Mater.* **2008**, *20*, 1230.
(11) Climent, M. J.; Corma, A.; Iborra, S.; Epping, K.; Velty, A. *J. Catal.* **2004**, *225*, 316.
(12) Benito, P.; Labajos, F. M.; Rives, V. *Cryst. Growth Des.* **2006**, *6*, 1961.
(13) Benito, P.; Herrero, M.; Barriga, C.; Labajos, F. M.; Rives, V. *Inorg. Chem.* **2008**, *47*, 5453.

Published on Web 11/20/2009

interesting proposal was the coprecipitation in alcoholic solution for the preparation of colloidal LDHs.[14,15]

An alternative that has received some attention in the past few years is the sol−gel method.[16−23] This method has several advantages over other synthetic procedures. It is a simple way to obtain nanoscaled particles, which have proven to be important for many of the new applications of LDHs; for instance, for the successful casting of LDH thin films. Also, high-purity products can be obtained; and the conditions throughout the process are mild, thus enabling an eventual intercalation of delicate organic molecules and biological species. Furthermore, the sol−gel method allows accurate control over structural and textural properties of the products; materials with high specific surface area and narrow pore size distribution can be obtained. A few methods have been reported for the sol−gel synthesis of MgAl,[16−18,20−23] MgGa,[20] MgIn,[20] NiAl,[18] and ZnAl[19] LDHs.

The authors have reported previously the synthesis of MgAl LDHs by a sol−gel technique;[22] the crystallization and particle growth mechanisms of these materials have also been studied.[23] This method has now been generalized to enable the synthesis of binary and ternary LDHs with virtually any chemical composition; it is, to the best of the authors' knowledge, the first time that such a general sol−gel method is presented.

An appropriate sol−gel method, that enables the synthesis of pure LDHs with tunable chemical compositions, must consider certain crucial parameters, such as the polarity, reactivity, and amount of the intended solvent, generally an alcohol.[22] Also, the quantity of water is essential to control the hydrolysis reactions. Additionally, the different reactivities of metal alkoxides should be taken into account. These are associated with the different Lewis acidities of the metals; and to the tendency of the metal atom to satisfy its higher coordination state.[24,25] Metal complexation with acetic acid, trifluoroacetic acid, acetylacetonates, and other chelating ligands has been used as a simple way to control the reactivity of inorganic precursors.[22−28] All the aforementioned synthesis parameters are discussed and analyzed.

Furthermore, the sols were successfully cast as thin films and catalytic membranes on glass and cordierite substrates, respectively. The development of LDH thin films permits an extensive diversity of applications; for instance, in optics, as functional coatings and membranes, for the development of sensing devices, as catalysts in microreactor coatings, in the development of organic−inorganic nanocomposites, for the preparation of CO_2-selective membranes and films,[29] etc.

There have been a number of different approaches to obtain LDH films,[14,15,29−35] e.g., surface precipitation,[30] the layer-by-layer method,[31] and electrochemical methods.[32,33] In another approach, binary LDHs were synthesized by coprecipitation in alcoholic solution, to obtain a colloidal suspension, from which thin films were obtained.[14,15] Also, self-supporting LDH films were prepared by a methodology denominated "separate nucleation and aging steps", which involves the use of a colloid mill to obtain colloidal LDH particles.[34] Another technique was the fabrication of an amorphous sol−gel-derived coating, followed by heat treatment and hot water immersion to obtain ZnAl LDH films.[35] Exfoliation has also been proposed as an alternative to produce LDH thin films.[36,37]

Sol−gel thin films have a number of advantages over other coating methods. For instance, large substrates may be accommodated, and it is possible to uniformly coat substrates such as pipes, tubes, rods and fibers that are not easily handled by other coating methods. Compared to conventional thin film forming processes such as chemical vapor deposition, evaporation or sputtering, sol−gel requires considerably less equipment and is less expensive. Also, sol−gel processing has the ability to control precisely the microstructure of the deposited film.[26] Because of this, thin films and coatings were the first successful commercial application of sol−gel products, and are still the most technologically important aspect of sol−gel processing.[26,38]

In this paper, a general sol−gel procedure to obtain multimetallic LDHs is developed, and the main synthesis

(14) Gardner, E.; Huntoon, K. M.; Pinnavaia, T. *J. Adv. Mater.* **2001**, *13*, 1263.
(15) Gursky, J. A.; Blough, S. D.; Luna, C.; Gomez, C.; Luevano, A. N.; Gardner, E. A. *J. Am. Chem. Soc.* **2006**, *128*, 8376.
(16) Lopez, T.; Bosch, P.; Ramos, E.; Gomez, R.; Novaro, O.; Acosta, D.; Figueras, F. *Langmuir* **1996**, *12*, 189.
(17) Lopez, T.; Bosch, P.; Asomoza, M.; Gomez, R.; Ramos, E. *Mater. Lett.* **1997**, *31*, 311.
(18) Prinetto, F.; Ghiotti, G.; Graffin, P.; Tichit, D. *Microporous Mesoporous Mater.* **2000**, *39*, 229.
(19) Tichit, D.; Lorret, O.; Coq, B.; Prinetto, F.; Ghiotti, G. *Microporous Mesoporous Mater.* **2005**, *80*, 213.
(20) Aramendia, M. A.; Borau, V.; Jimenez, C.; Marinas, J. M.; Ruiz, J. R.; Urbano, F. J. *J. Solid State Chem.* **2002**, *168*, 156.
(21) Bolognini, M.; Cavani, F.; Scagliarini, D.; Flego, C.; Perego, C.; Saba, M. *Microporous Mesoporous Mater.* **2003**, *66*, 77.
(22) Valente, J. S.; Cantu, M. S.; Cortez, J. G. H.; Montiel, R.; Bokhimi, X.; Lopez-Salinas, E. *J. Phys. Chem. C* **2007**, *111*, 642.
(23) Valente, J. S.; Prince, J.; Maubert, A. M.; Lartundo-Rojas, L.; Angel, P.; Ferrat, G.; Hernandez, J. G.; Lopez-Salinas, E. *J. Phys. Chem. C* **2009**, *113*, 5547.
(24) Aegerter, M. A.; Jafelicci, M., Jr.; Souza, D. F.; Zanotto, E. D. *Sol−Gel Sci. Technol.* World Scientific Publishing Co Pte Ltd., Singapore, 1989.
(25) Schubert, U. *Acc. Chem. Res.* **2007**, *40*, 730.
(26) Brinker, J.; Scherer, G. *Sol−Gel Science: The Physics and Chemistry of Sol−Gel Processing*; Academic Press: New York, 1989.
(27) Fan, J.; Boettcher, S. W.; Stucky, G. D. *Chem. Mater.* **2006**, *18*, 6391.
(28) Boettcher, S. W.; Fan, J.; Tsung, C.-K.; Shi, Q.; Stucky, G. D. *Acc. Chem. Res.* **2007**, *40*, 784.
(29) Kim, T. W.; Sahimi, M.; Tsotsis, T. T. *Ind. Eng. Chem. Res.* **2009**, *48*, 5794.
(30) Gao, Y. F.; Nagai, M.; Masuda, Y.; Sato, F.; Seo, W. S.; Koumoto, K. *Langmuir* **2006**, *22*, 3521.
(31) Lee, J. H.; Rhee, S. W.; Jung, D. Y. *J. Am. Chem. Soc.* **2007**, *129*, 3522.
(32) Scavetta, E.; Mignani, A.; Prandstraller, D.; Tonelli, D. *Chem. Mater.* **2007**, *19*, 4523.
(33) Yarger, M. S.; Steinmiller, E. M. P.; Choi, K. S. *Inorg. Chem.* **2008**, *47*, 5859.
(34) Wang, L.; Li, C.; Liu, M.; Evans, D. G.; Duan, X. *Chem Commun.* **2007**, 123.
(35) Yamaguchi, N.; Nakamura, T.; Tadanaga, K.; Matsuda, A.; Minami, T.; Tatsumisago, M. Cryst. Growth Des., **2006**, Vol. *6* No. 7, 1726.
(36) Ma, R.; Liu, Z.; Takada, K.; Iyi, N.; Bando, Y.; Sasaki, T. *J. Am. Chem. Soc.* **2007**, *129*, 5257.
(37) Li, L.; Ma, R.; Ebina, Y.; Iyi, N.; Sasaki, T. *Chem. Mater.* **2005**, *17*, 4386.
(38) Mahltig, B.; Haufe, H.; Bottcher, H. *J. Mater. Chem.* **2005**, *15*, 4385.

parameters are discussed; crystalline structure, morphology, thermal decomposition and textural properties of various multimetallic sol−gel LDHs were studied. In addition, the structure, orientation, uniformity and thickness of the LDH thin films were investigated, as well as methods for control over film thickness. The development of thin films is merely one application, out of the multiple possibilities that this method enables.

2. Experimental Section

2.1. Synthesis of MgAl LDH. The synthesis of MgAl LDHs was reported previously.[22,23] Briefly, aluminum trisec-butoxide (ATB) was dissolved in ethanol and refluxed under constant stirring for one hour. Nitric acid solution (3 M) was then slowly added. After 1 h, the system was taken to room temperature, and acetic acid (AA) was added. One hour later, the temperature was lowered to 0 °C, and magnesium methoxide was added dropwise. The system was taken to room temperature and maintained in constant stirring for 18 h. Finally, water was added to reach the desired molar ratio. The molar ratios of reactants were ATB:EtOH = 1:60, ATB:HNO_3 = 1:0.03, ATB:AA = 1:1, Mg:Al = 3:1, H_2O:ATB = 1:1.

2.2. Synthesis of Other Binary and Ternary LDHs. The synthesis procedure for LDHs with different compositions from MgAl remains the same as above, up to the point of AA addition. After lowering the temperature to 0 °C, a solution of the metallic precursor in ethanol (0.3 M) was added dropwise. For ternary LDHs, the cation in larger proportion was added first, and the second cation (10 or 15% wt.) was added one hour later, maintaining the system at 0 °C. Then, it was taken to room temperature and maintained in constant stirring for 18 h.

Finally, the sols were either dried at 70 °C for 24 h to obtain a powder, or aged at room temperature for 7 days to obtain a transparent gel. The molar ratios of reactants in this case were ATB:EtOH = 1:60, ATB:HNO_3 = 1:0.03, M^{II}:M^{III} = 3:1. The H_2O/ATB molar ratio was determined by the number of hydration water molecules in the metal precursors and the addition of water contained in the HNO_3 solution. The AA/ATB ratio was varied between 1 and 3, depending on the reactivity of the metal precursors and the total H_2O/ATB ratio. For details on the amounts and reagents employed for each sample, see the Supporting Information.

LDH samples were named according to their composition; e.g., MgAl stands for a magnesium−aluminum LDH. In ternary LDHs, the cation in larger proportion is mentioned first. In sample NiCoAl, cobalt acetate was used as precursor; it was dissolved in methanol, as it is not sufficiently soluble in ethanol. Two different NiAl LDHs were synthesized, using nickel acetate (NiAl-A), or a mixture of nickel acetate (33% mol) and nickel nitrate (67% mol) (NiAl-N), in order to determine the effect of precursor salt. Aged sols were named (M)Al-*X*d, where *X* indicates the aging time of the sol in days.

2.3. Production of Gels, Thin Films, and Catalytic Membranes. The sols were aged at room temperature for 7 days, on an open vessel without stirring, to obtain transparent gels. Thin films were formed by dip-coating using a glass slide, maintaining the substrate speed constant. The substrates were immersed in either as-prepared or aged sols. The film was placed in a covered glass beaker immediately after immersion as a way to control the deposition ambient and thus the evaporation rate.[26] Catalytic membranes were also prepared by dip-coating, using cordierite monoliths as substrate. The number of impregnations was varied between 1 and 5; the monolith was calcined at 500 °C after each impregnation.

2.4. Characterization Techniques. *Transmission Electron Microscopy*. Powdered samples were analyzed through transmission electron microscopy (TEM) in a Jeol 200 Kv JEM-2200FS. The microscope is equipped with a Schottky-type field emission gun in ultra high-resolution (UHR) configuration (Cs = 0.5 mm; *Cc* 1.1 mm; point-to-point resolution, 0.19 nm) and in-column omega-type energy filter. Samples were dispersed in ethanol before placing them on the copper grid with Formvar support.

Powder X-ray Diffraction. The X-ray patterns were measured in a D-500 diffractometer, with Cu $K\alpha_{1,2}$ radiation, and a graphite secondary beam monochromator. The diffraction patterns were measured from 4 to 80° 2θ using a step size of 0.02° and step scan of 2 s.

Thermal Gravimetric Analysis. Thermogravimetric (TG) analyses were carried out on a Netzch STA-409 EP equipment, which was operated under a helium flow at a heating rate of 10 °C/min from 25 to 1000 °C. In all determinations, 100 mg of finely powdered dried HT sample was used.

Infrared Spectroscopy. Diffuse reflectance infrared Fourier transform (DRIFT) spectra of powdered solids were recorded using a Bruker Equinox 55 spectrometer equipped with a Harrick diffuse reflection attachment (H-DRP-BR-3) and a Harrick reaction chamber (HVC-DR2). Spectra were taken using a DLATGS high sensibility detector over the ranges of 4000−400 cm^{-1} with a resolution of 4 cm^{-1}, and 300 scans were collected. Prior to analyses, samples were diluted to 5 wt %with KBr. Samples were heat treated in situ from room temperature to 500 °C, under a helium flow of 5 mL min^{-1}. Spectra were collected at 50 °C intervals, allowing the sample to stabilize for 1 h at each temperature.

Textural Analysis. The texture of the calcined powdered samples (at 500 °C/4 h in air) was analyzed by N_2 physisorption at −196 °C on an AUTOSORB-I apparatus. Prior to the analysis, the samples were outgassed in a vacuum (1×10^{-5} Torr) at 400 °C for 5 h. The surface areas were calculated by using the Brunauer−Emmett−Teller (BET) method, and the pore size distribution and total pore volume were determined by the Brunauer−Joyner−Hallenda (BJH) method applied to the desorption branch.

Film X-ray Diffraction. The XRD measurements of the films were performed on a D8 Discover equipment from Bruker AXS furnished with a General Area Diffraction Detection System (GADDS). The configuration consisted of Cu $K\alpha_{1,2}$ radiation, X-ray beam size of 500 μm, Göbel mirror monochromator, a laser beam-light microscopy and a HI-STAR area detector. A high-resolution configuration was selected and the detector was fixed at 30 cm for detecting 17.5° 2θ. The diffraction patterns were obtained as a grazing incident beam technique (GIBT) in order to measure the LDH film deposited on the glass substrate surface.

Scanning Electron Microscopy and Energy-Dispersive X-ray Spectroscopy. Scanning electron microscopy (SEM) was used to characterize the thin films and catalytic membranes, in a Phillips XL 30 environmental SEM. The chemical composition and bidimensional spatial distribution of the film and the substrate was examined by X-ray Mapping using an energy-dispersive X-ray spectrometer (EDS) device attached to the microscope. Samples were prepared by cutting the glass slides into rectangular sections of 5×8 mm^2, using a ceramic blade. Samples were fixed onto a 90° sample holder using colloidal silver.

3. Results and Discussion

3.1. Main Synthesis Parameters. Proposing a reaction mechanism in sol−gel synthesis is challenging, as the

different species that may be formed are quite numerous. However, it is possible to describe the various steps during the synthesis and analyze the influence that each parameter has on the final product.

Aluminum alkoxides are highly reactive when compared to silicon alkoxides, because of the larger difference in electronegativity between Al and O, and the consequent polarization of the Al−O bond; also, the higher coordination number of aluminum increases its reactivity.[24] Furthermore, because of the high Lewis acidity of Al, aluminum alkoxides show large affinity to form oligomers $[Al(OR)_m]_n$ with alkoxo bridges between two or three metal atoms, i.e., by interaction of the Lewis basic alkoxo groups with the metal centers. The physical properties as well as the chemical reactivity of the metal alkoxides are influenced by the degree of oligomerization.[25] Aluminum tri-*sec*-butoxide was chosen because the large size and ramification of the alkyl group provides steric hindrance to the formation of coordination linkage, a first way to control reaction rates. Initially, aluminum tri-*sec*-butoxide is dissolved in ethanol and alcoholysis reactions take place:

$$Al(OsBu)_3 + x\mathrm{EtOH} \rightarrow Al(OsBu)_{3-x}(OEt)_x + x(s\mathrm{BuOH}) \quad (1)$$

Because of the large *sec*-butoxi group, facility of exchange of alkoxy groups is largely diminished. However, the original alkoxide reactivity is enhanced by this reaction. Afterward, by the addition of a limited amount of water in a nitric acid solution, partial hydrolysis reactions take place

$$Al(OR)_3 + xH_2O \rightarrow Al(OR)_{3-x}(OH)_x + x(\mathrm{ROH}) \quad (2)$$

Here, R may be an ethyl or *sec*-butyl radical. The metal−alkoxide bond is extremely susceptible to hydrolytic reactions, so this reaction is completed rapidly; moreover, this reaction is catalyzed by H^+. Upon hydrolysis, the reaction mixture becomes completely transparent, because the alkoxo bridges between $[Al(OR)_m]_n$ oligomers are broken. Acetic acid is then introduced in the reaction medium, which will act as a complexing agent by hindering future hydrolysis reactions.[24] Metal alkoxides generally undergo facile reactions with acetic acid, as follows

$$Al(OR)_3 + xCH_3COOH \rightarrow Al(OR)_{3-x}(CH_3COO)_x + x(\mathrm{ROH}) \quad (3)$$

In this way, hydrolysis, condensation and extended polymerization are controlled. The carboxylate moiety binds the metal in a variety of ways, mainly: monodentate, bidentate bridging and bidentate chelating (Supporting Information). Bidentate ligands are more strongly bonded than the corresponding monodentate ligands, and are less readily hydrolyzed than the remaining OR groups upon sol−gel processing.

In addition to the fact that the acetate-modified precursor has a different reactivity, the degree of cross-linking of the gel network is decreased, because of the smaller proportion of hydrolyzable OR groups. The substitution of monodentate alkoxy by bidentate acetate lowers the connectivity of the molecular building blocks. This favors the formation of gels instead of crystalline precipitates.[39] Also, it is likely that a substantial amount of acetates are retained in the gels. This might give one the ability to introduce organic anions in the interlayer galleries, by means of appropriately substituted acetate derivatives.[39]

During the synthesis of MgAl LDHs reported previously,[22,23] an acetic acid/aluminum (AA/ATB) molar ratio of 1 was found to be enough for the complexation of aluminum alkoxide. Substoichiometric amounts of water were used, so hydrolysis reactions were more easily controlled. In multimetallic LDHs, the addition of excess water, contained as crystallization water in the metallic salt precursors, is inevitable. Therefore, hydrolysis and condensation reactions must be hindered by adding larger amounts of acetate as complexing agent. This can be done by either using acetate precursors or adding more acetic acid.

When using nitrate salts (e.g. zinc nitrate, copper nitrate, etc.), the AA/ATB molar ratio was raised to 3. It has been reported that aluminum alkoxide reactions with acetic acid occur in two stages; the first two substitutions are fast, whereas the third is very slow.[24] Hence, it is reasonable to assume that, when using an AA/ATB ratio of 3, approximately 1/3 of the acetic acid will remain unreacted, which will then complex the metallic salts that are introduced in the next stage.

Excess acetic acid leads to the in situ formation of acetate salts. In some cases, this is undesirable; for instance, in cobalt-containing LDHs, as cobalt acetate is not sufficiently soluble in ethanol. For the preparation of sample NiCoAl, cobalt acetate was dissolved in methanol, and LDH phase was easily obtained. On the other hand, for the synthesis of sample CoNiAl, cobalt nitrate was employed as precursor. A test was performed using an AA/ATB ratio of 3, resulting in mixed LDH and cobalt acetate phases (data not shown). Therefore, in this case, pure LDH phase was obtained only when using a ratio AA/ATB = 1.

The choice of metallic precursors is based solely on their solubility.[24] Any salt with a suitable solubility in an alcohol may be employed. The amount of acetic acid that is needed is then determined based on the reactivity and amount of hydration water in each precursor. In this simple way, this method may be extended to prepare LDHs with chemical compositions other than those presented here.

By the time that the second (and third) metal is added, the reaction medium contains a number of different species, such as aluminum alkoxides, acetates and hydroxides, in different proportions. Their reactivity varies as: hydroxide > ethoxy > *sec*-butoxi ≫ acetates. Condensation reactions begin to take place, slowed down by acetate groups and by the slightly acidic pH. Under these conditions, controlled condensation occurs, and an LDH is

(39) Schubert, U. *J. Mater. Chem.* **2005**, *15*, 3701.

formed, instead of two or more separate hydroxide phases. At this stage, the following reactions take place

$$M(OR)_n + M'(CH_3COOH)_m \rightarrow (RO)_{n-1}-M-O-M'-(CH_3COO)_{m-1} + CH_3COOR \quad (4)$$

$$M(OH)_n + M'(OH)_m \rightarrow (OH)_{n-1}-M-O-M'-(OH)_{m-1} + H_2O \quad (5)$$

$$M(OH)_n + M'(OR)_m \rightarrow (OH)_{n-1}-M-O-M'-(OR)_{m-1} + ROH \quad (6)$$

Here, M and M′ represent two different metals (e.g. aluminum and magnesium), whereas R is an alkyl radical (ethyl, *sec*-butyl, etc.). This process goes on with oligomerization and then polymerization reactions, increasing the connectivity of the network. Finally, if the sols are aged at room temperature, slow solvent evaporation and continued polymerization lead to the formation of gels.[24] Photographs of transparent gels, formed after aging the sol, can be found in the Supporting Information.

In previous attempts at synthesizing LDHs by a sol−gel method, pH was adjusted to ∼10 by adding a base such as NH_4OH.[16−20] Presumably, this was done because high pH is indispensable in the synthesis of LDHs by the traditional coprecipitation route. It is therefore worth noting that in sol−gel synthesis, the mechanism of formation is not by precipitation of cations, which occurs at high pH; but by slow condensation reactions of the partially hydrolyzed metal cations, which can be controlled at slightly acidic pH.

3.2. Morphology, Crystalline Structure and Crystallographic Size. Previous transmission electron microscopy (TEM) studies on MgAl LDHs prepared with different alcohols as solvent revealed a very particular nano core−shell or nanocapsular morphology, regardless of the alcohol.[22] This is a great contrast from the traditional platelet-like morphology obtained by different methods such as coprecipitation,[11] urea hydrolysis,[13] and microwave irradiation.[11,12] It was later determined that upon hydrothermal treatment with the mother liquor (ethanol), the capsules coalesce and grow; if excess water is added before hydrothermal treatment, they aggregate and form very ordered platelets with a high degree of crystallinity.[23] Furthermore, it was found that the nanocapsular morphology is metastable and restricted to nonaqueous systems.[23]

All binary and ternary LDHs prepared by this method reveal similar nanocapsular morphology. TEM in Figure 1 shows what appears to be rings, that in fact are hollow capsules, for representative samples (a) MgAl, (b) NiAl-A, (c) NiCoAl, and (d) NiAl-N. High-resolution microscopy revealed that the capsule's shell is lamellar, see insets in Figure 1. It is worth noting that the formation of these capsules is not restricted to alkoxide precursors, and the morphology does not change with the use of acetate or nitrate salts. Capsule size, on the other hand, is affected by the precursor salt. For MgAl, size ranges from 10 to 40 nm; for NiAl-N, it is between 5 and 15 nm; and for NiAl-A and NiCoAl, capsules' size is ≤5 nm. It appears that, upon increasing acetate amount (acetate/aluminum molar ratios are 1, 3, 7, and 7 for MgAl, NiAl-N, NiAl-A, and NiCoAl, respectively; see the Supporting Information), capsules become smaller. This is very likely due to the fact that acetate lowers the connectivity of molecular building blocks;[39] consequently, smaller particles are obtained. It should then be possible to control particle size by varying the acetate amount for a given composition.

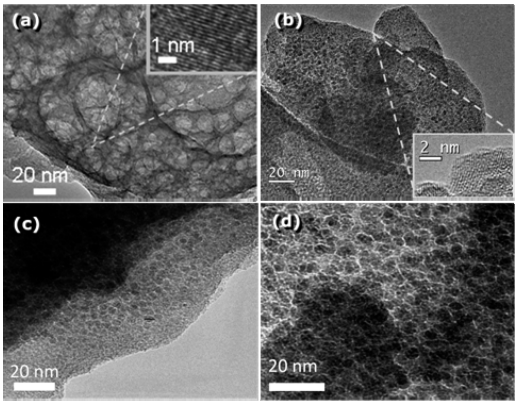

Figure 1. TEM images of sol−gel LDHs: (a) MgAl, (b) NiAl-A, (c) NiCoAl, (d) NiAl-N.

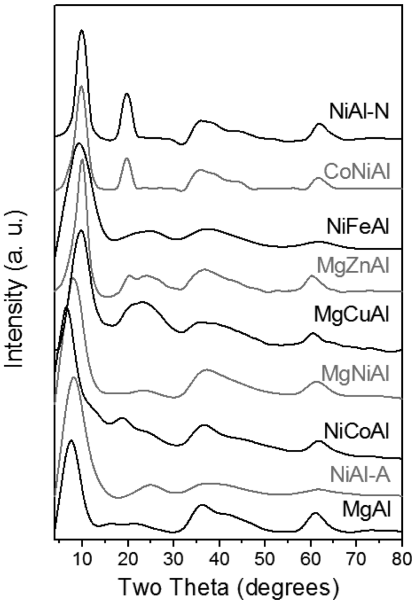

Figure 2. XRD patterns of sol−gel LDHs.

In such small particles, the chemistry is dominated by the surface atoms, as they represent a larger portion of the total structure. Atoms in surfaces, edges and corners are not fully coordinated, and therefore are more reactive.[15] LDH nanoparticles have shown remarkable properties, such as increased catalytic activity[40] and fire retardant properties.[41] They are also of particular interest in

(40) Choudary, B. M.; Jaya, V. S.; Reddy, B. R.; Kantam, M. L.; Rao, M. M.; Madhavendra, S. S. *Chem. Mater.* **2005**, *17*, 2740.
(41) Wang, Z.; Han, E.; Ke, W. *Prog. Org. Coatings* **2005**, *53*, 29.

Table 1. Cell Parameters, Crystal Sizes, and Textural Properties of Sol−Gel LDHs

	cell params (Å)		cryst size (nm)				
sample	*c*	*a*	L_{003}	L_{110}	S_{BET}(m^2 g^{-1})	pore volume (cm^3 g^{-1})	pore diameter (nm)
MgAl	34.989	3.041	2	6	289	0.812	7 and 42
NiAl-A	37.091	3.009	2	6	271	0.204	3
NiCoAl	41.432	3.005	3	8	214	0.277	3
MgNiAl	33.574	3.037	3	6	290	0.217	3
CoNiAl	27.582	3.007	8	9	111	0.156	4
MgCuAl	26.222	3.069	2	6	121	0.099	2 and 11
NiFeAl	27.930	3.036	2		143	0.154	4
MgZnAl	27.022	3.045	4	5	200	0.126	3
NiAl-N	26.616	2.997	3	6	270	0.243	4

the fields of bionanotechnology[42] and nanocomposite materials.[43]

XRD patterns of the samples are presented in Figure 2, showing the characteristic peaks of an LDH structure, with broader peaks that are indicative of low crystallinity. Also, the capsular morphology may have a widening effect on XRD peaks,[22] because of the tension generated by the bend of the layers. The positions of the 00*L* reflections are shifted to lower 2θ relative to a traditional MgAl-CO_3 because of the expansion of the interlayer region by the intercalation of larger anions. Cell parameters *c* and *a*, related to the interlayer spacing and the average cation−cation distance, were calculated considering 3*R* stacking (Table 1). Here, the effect of precursor salt becomes evident. Samples prepared only with alkoxides and/or acetates (MgAl, NiAl-A, NiCoAl, MgNiAl) have larger interlayer spacing than those prepared using both nitrates and acetates/alkoxides. It appears that, when nitrates are present in the reaction medium, they are preferably intercalated and displace other anions such as alkoxys and acetates. It has been determined that the affinity of LDHs for NO_3^- as interlayer anions is relatively high; it is only surpassed by halogen, hydroxyl, sulfate, and carbonate anions.[44]

Crystal sizes, calculated by the Scherrer equation applied to the 003 and the 110 reflections, are < 10 nm in all cases (Table 1). Crystal and particle sizes, as well as morphology, can be modified by hydrothermal treatments, as the authors have previously demonstrated on sol−gel MgAl LDHs.[23] Changes in crystallinity and morphology also alter the physicochemical properties of the samples. Therefore, these properties can be fine-tuned according to the intended applications.

3.3. Thermal Decomposition Behavior. Thermal gravimetric analyses of traditional coprecipitated MgAl-CO_3 LDHs commonly show three weight loss intervals: (i) between room temperature and 250 °C, crystallization water, weakly bound OH groups and physisorbed CO_2 are lost; (ii) from 250 to 450 °C, there occurs the loss of most interlayer anions and the dehydroxylation of brucite-like sheets; and (iii) above 450 °C, there is generally a small loss, corresponding to strongly bound interlayer anions.[22,45] In DTA profiles the first two events are accompanied by two endothermic peaks. The first one, more intense, is usually centered at ~ 220 °C; the second one is broad, with two components at 330 and 380 °C. An additional, endothermic peak may appear below 100 °C if the sample is hydrated.[2]

The thermal decomposition of the sol−gel MgAl LDH resembles that of its coprecipitated analogue. It was studied previously by TGA-DTA analyses and mass spectroscopy,[22] revealing that, up to 250 °C, mostly water and OH groups were lost, with a small contribution of CO_2 and C_xH_y fractions; the weight loss in this interval was 16.7%. Between 250 and 450 °C, 21.4 wt % was lost, corresponding to H_2O, OH, CO_2 and a significant contribution of organic fragments, C_xH_y. From these results, it was determined that interlayer anions were mainly ethoxy groups, from ethanol that was used as solvent, along with a small amount of CO_3^{2-} trapped from the ambient. Furthermore, between 450 and 650 °C, there was a smaller loss of 2.3 wt %, corresponding to H_2O, OH, CO_2, and C_xH_y fragments.[22] DTA profiles revealed two endothermic peaks at ~ 75 and 360 °C.

The TGA-DTA profiles of the multimetallic sol−gel LDHs are presented in Figure 3. The weight loss intervals of these samples are similar to those of sol−gel MgAl LDH. The first decomposition step, corresponding to the loss of H_2O and OH groups, ends at temperatures ≤200 °C, at least 50° less than in a coprecipitated MgAl-CO_3. This may be related to the small crystal size of multimetallic sol−gel LDHs; if crystals are smaller, water molecules are nearer to the layers' edges, and leave more easily, for they encounter less diffusional problems. Weight losses at this stage varied from 7.6% for NiFeAl to 20.9% for MgZnAl. The DTA curves of all samples show an endothermic minimum around 120−150 °C.

The second stage (~200−450 °C) corresponds to the decomposition of interlayer anions. In this interval there are significant differences among the samples, regarding the weight percentage that is lost in each case, the TGA curves slopes, and the DTA profiles. This behavior is explained by the variety of anions that were initially present in the reaction medium. They may include NO_3^-, CO_3^{2-}, acetates, and alkoxy groups, depending on the metallic precursors used for each sample (see the Supporting Information). Any of these molecules may be intercalated as charge-compensating anions; their relative

(42) Xu, Z. P.; Zeng, Q. H.; Lu, G. Q.; Yu, A. B. *Chem. Eng. Sci.* **2005**, *61*, 1027.
(43) Pavan, P. C.; Cardoso, L. P.; Crepaldi, E. L.; Valim, J. B. *Stud. Surf. Sci. Catal.* **2000**, *129*, 443.
(44) Miyata, S. *Clays Clay Miner.* **1983**, *31*, 305.
(45) Vágvölgyi, V.; Palmer, S. J.; Kristóf, J.; Frost, R. L.; Horváth, E. *J. Colloid Interface Sci.* **2008**, *318*, 302.

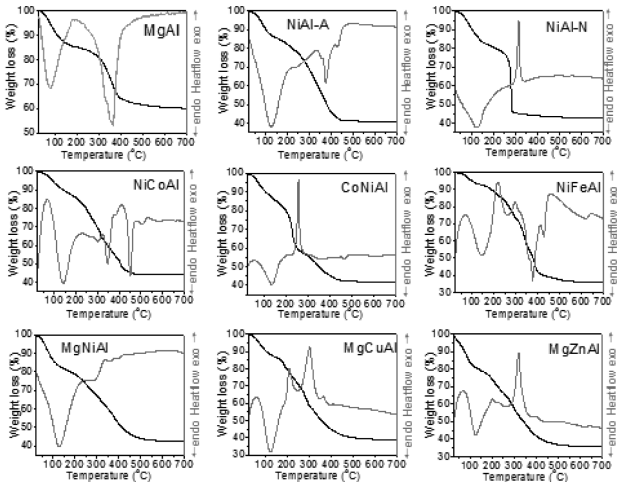

Figure 3. TGA-DTA profiles of sol−gel LDHs.

amounts depend on the affinity of LDHs for each anion and the chemical composition. This is in agreement with the variation of interlayer distances, which indicated that each sample has different interlayer anions, as discussed above. Weight losses at this stage ranged from 34 wt % for MgNiAl to 53 wt % for NiFeAl.

The effect of interlayer anions can be directly determined by comparing two samples with the same chemical composition and very similar crystal sizes, samples NiAl-A (prepared using nickel acetate) and NiAl-N (prepared with a mixture of nickel acetate and nickel nitrate). It is interesting to note that, whereas NiAl-A loses anions gradually by an endothermic process, sample NiAl-N shows an abrupt weight loss at ~300 °C accompanied by a strong exothermic event.

In fact, exothermic events were observed only in samples NiAl-N, CoNiAl, NiFeAl, MgCuAl, and MgZnAl, which were prepared using both nitrates and an organic precursor (acetate and/or alkoxide), and thus have them as charge-balancing anions (see the Supporting Information). This behavior can be explained by the fact that nitrates provide the required oxygen for the exothermic combustion of the organic precursor. Furthermore, among nitrate-containing samples, the exothermic signal is much stronger when there are acetates (CoNiAl, NiAl-N) than when there are only alkoxides (MgCuAl, MgZnAl) as organic compounds. NiFeAl LDH may be considered an exception because the nitrate/acetate ratio is much lower in this sample. On the other hand, when only alkoxides and acetates were used as precursors (samples MgAl, NiAl-A, NiCoAl, and MgNiAl), the interlayer anions decompose endothermically at different temperatures.

Another comparison may be drawn between samples NiAl-A and NiCoAl, which were both prepared using aluminum alkoxide and metal acetates. Therefore, presumably, they both have the same interlayer anions. Their weight losses in the 200−450 °C intervals are very comparable. However, NiCoAl has an additional endothermic minimum at 450 °C, when compared to NiAl-A. This difference may be ascribed to the larger crystal sizes of

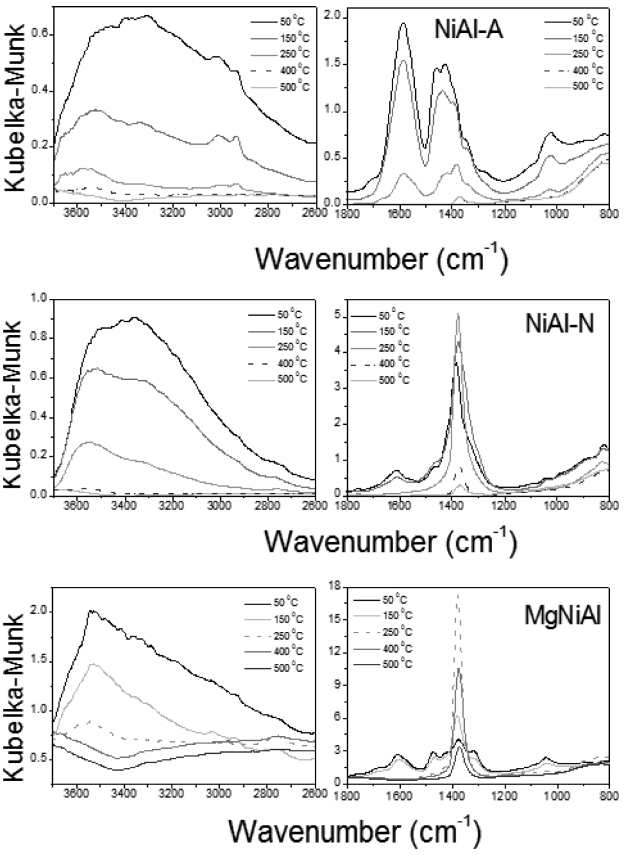

Figure 4. Infrared spectra of sol−gel samples, recorded at the indicated temperatures.

NiCoAl (see Table 1). As mentioned previously, larger crystals imply more diffusion problems for the departing anions. Also, the strength by which anions are bound is strongly dependent on chemical composition.

To better understand the decomposition processes of multimetallic sol−gel LDHs, we thermally treated samples in situ and recorded the IR spectra at different temperatures. Select spectra for samples NiAl-A, NiAl-N, and MgNiAl at 50, 150, 250, 400, and 500 °C are shown in Figure 4. These three samples were chosen because they allow studying the effect of interlayer anion (NiAl-N vs NiAl-A) and the effect of chemical composition.

In the OH region, between 3900 and 2700 cm^{-1}, all samples had similar behavior. At 50 °C, there is a strong, wide band around 3450 cm^{-1}, typical of hydrogen-bonded OH groups in LDH layers. This band may result from the overlapping of two, or even three, OH stretching vibrations, and one vibration due to interlayer water.[2] Upon heating, the OH vibrations decrease substantially. At 400 °C, nearly all OH groups apparently have been removed.

Also in this region, sample NiAl-A has two small peaks at ~3016 and 2936 cm^{-1} that correspond to antisymmetric and symmetric CH_3 stretching, respectively.[46] These bands may arise from acetates and/or alkoxy groups, and are not present in either NiAl-N or MgNiAl.

(46) Nakamoto, K. *Infrared and Raman Spectra of Inorganic and Coordination Compounds*, 5th ed.; John Wiley & Sons: New York, 1997.

In the region between 1800−800 cm^{-1} (Figure 4), NiAl-A has two strong bands at 1587 and 1460 cm^{-1}, which correspond to ν_a (COO) and ν_s (COO) of acetate groups. The bonding mode of the carboxylate ligand can be identified by the difference between asymmetric and symmetric stretching frequencies. In this case, $\Delta = \nu_a - \nu_s = 127$ cm^{-1} corresponds to a bidentate chelating ligand (see the Supporting Information).[46,47] Another band appears at 1425 cm^{-1}, which could be ascribed to interlayer bicarbonate. However, the presence of interlayer bicarbonate in large amounts is unlikely; given the intensity of this band, it is more probable that it belongs as well to ν_s COO of acetate groups, bonded as a bidentate bridging ligand ($\Delta = 162$ cm^{-1}). These three bands diminished their intensity at increasing temperatures, and completely disappeared at 400 °C. The similar thermal behavior of the three bands supports the idea that they all come from acetate groups in different binding modes. The CH_3 bands observed at 3016 and 2936 cm^{-1} disappeared at the same temperature as the COO bands, suggesting that they come from acetate as well. Also, there is a characteristic band at ~1000 cm^{-1} from C−O in alkoxy groups, which is no longer detected at 400 °C.[46]

Also in NiAl-A, two small shoulders are present at ~1380 and 1350 cm^{-1}, which arise from CO_3^{2-} in D_{3h} planar symmetry.[2] Carbonate anions are most likely trapped from the ambient during synthesis, as LDHs are known for their great affinity for CO_2. The band at 1380 cm^{-1} is present even after annealing at 500 °C, indicating that CO_3^{2-} is strongly adsorbed on basic sites. Accordingly, TGA results show that this sample continues to lose weight up to 650 °C.

In sample NiAl-N (Figure 4), the most prominent band is located at ~1380 cm^{-1}. It could belong to either the ν_3 mode of CO_3^{2-}, or to the antisymmetric stretching mode of NO_3^-.[46] Most likely, it is an overlapping of these two bands, considering its broadness and asymmetry; the main contribution should be from the nitrate groups. The intensity of this band increased slightly with temperature, reaching a maximum at 250 °C, and then decreased drastically. It is very possible that CO_2 is formed by the decomposition of organic anions, and is then adsorbed as carbonate on the basic sites of the LDH.

Another band at 822 cm^{-1} belongs to the out-of-plane symmetric deformation mode of NO_3^-.[2] The small band at 1610 cm^{-1} and a shoulder at 1466 cm^{-1} are ascribed to acetate groups acting as a bidentate chelating ligand. These bands are no longer observed at 250 °C. Even though acetates are also present in this sample, they have been largely displaced by nitrate anions, in accordance with the interlayer spacing observed by XRD, which was smaller than that of NiAl-A. Finally, the small band at 1040 cm^{-1} that disappears at 400 °C corresponds to alkoxy groups.[46]

MgNiAl has behavior similar to that of NiAl-N. At 50 °C, there are four main bands: two are located at 1609 and 1472 cm^{-1}, which correspond to bidentate chelating acetate ($\Delta = 137$ cm^{-1}); another at 1379 cm^{-1}, assigned to carbonate; and one more at 1043 cm^{-1}, from the C−O vibration of alkoxy groups.[46] As in NiAl-N, the intensity of the carbonate band increases with temperature up to 250 °C, and then decreases again. Another small band at 840 cm^{-1} appears at 250 °C, from the ν_2 vibration of CO_3^{2-}.[2] At 500 °C, there is still a significant amount of carbonate. In a qualitative sense, MgNiAl retains more carbonate at 500 °C than NiAl-A and NiAl-N; this may be related to the stronger basic sites created by $Mg^{2+}-O^{2-}$ pairs.

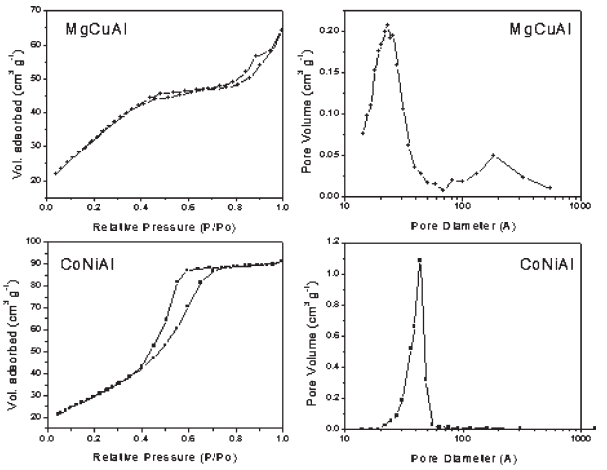

Figure 5. N_2 adsorption−desorption isotherms and corresponding BJH pore size distributions of indicated calcined samples.

3.4. Textural Properties. Nitrogen adsorption−desorption isotherms of calcined sol−gel LDHs (Figure 5 and the Supporting Information) are of type IV, which characterizes mesoporous solids, according to the IUPAC classification.[48] However, significant differences are appreciated in the shapes of hysteresis loops and in the pore size distributions. On the basis of these differences, samples may be divided in two groups. Figure 5 shows the isotherms and pore size distributions for MgCuAl, representative of the first group, and for CoNiAl, illustrative of the second group.

In the first group are calcined MgAl and MgCuAl, which have type H1 loops.[49] These samples have two distinct steps in their hysteresis loops, which indicate a bimodal pore size distribution. The first narrow hysteresis loop (in the range $0.6 < P/P_0 < 0.85$ for MgAl, and $0.4 < P/P_0 < 0.6$ for MgCuAl) evidence pores with a regular geometry, attributed to intraparticle porosity. The second hysteresis loop, in $P/P_0 \geq 0.8$, denotes meso- and macropores with a nonuniform distribution, from interparticle voids.[22] These results are in accordance with BJH pore size distributions, displayed as insets in Figure 5. The total pore volume is mainly due to the smaller pores with more homogeneous size distribution.

In the second group are all the other mixed oxides, obtained by calcination of multimetallic LDHs, which

(47) Deacon, G. B.; Phillips, R. J. *Coord. Chem. Rev.* **1980**, *33*, 227.
(48) Sing, K. S. W.; Everett, D. H.; Haul, R. A. W.; Moscou, L.; Pierotti, R. A.; Rouquerol, J.; Siemieniewska, T. *Pure Appl. Chem.* **1985**, *57*, 603.
(49) Rouquerol, F.; Rouquerol, J.; Sing, K. *Adsorption by Powders and Porous Solids*; Academic Press: London, 1999.

presented type IVb isotherms.[49] This type of isotherm is associated with complex pore structures, made up of interconnected networks of pores of different shapes. The steep desorption branch is dependent on network-percolation effects, opposed to the capillary condensation that causes the appearance of H1 (and other types) hysteresis loops. These type of isotherms are commonly found with inorganic oxide gels.[49] Similar isotherm shapes were reported previously in NiAl and MgAl sol−gel LDHs.[16,19] It has also been observed with silica xerogels made up of small globular units of uniform size (1−2 nm).[49] Therefore, the observed hysteresis loops are in agreement with the morphology of these sol−gel LDHs; the hollow nanocapsules, observed by TEM, collapse upon calcination, resulting in even smaller globular particles, and a mesoporous network is created by the irregular arrangement of these. The main difference between the samples of the first and second groups is their particle size, because the latter have a capsule size ≤15 nm, as observed by TEM.

Worth noticing is the narrow, unimodal pore size distribution of these solids (Figure 5 and the Supporting Information), which ranges from 3−4 nm. This is a marked contrast from calcined LDHs synthesized by coprecipitation or similar methods, which usually present a broad pore size distribution in the meso- and macropore range.[22]

Table 1 presents the textural properties of all sol−gel LDHs. BET surface area values range from 111 to 290 m^2 g^{-1}; pore volumes reached values as high as 0.89 cm^3 g^{-1}, for MgAl, and is approximately 0.1−0.2 cm^3 g^{-1} for multimetallic samples. Micropore volume was negligible in all cases (≤0.01 cm^3 g^{-1}).

3.5. Thin Films and Catalytic Membranes. Thin films and catalytic membranes were produced by dip-coating technique. For LDH thin films, glass was used as substrate; it was immersed once in the sol, then dried at room temperature for 24 h. Catalytic membranes were prepared on cordierite monoliths, with up to five immersions on the sol, calcining at 500 °C after each immersion.

Previous reports indicate that thin LDH films tend to develop a preferred orientation,[14,15,33,34] evidenced by XRD patterns with strong 00*L* (basal spacing) reflections, and the absence of in-plane reflections. This feature may have significant effects on film properties, especially since LDHs are anisotropic crystal structures. Two-dimensional image (background), obtained with HI-STAR area detector, and corresponding integrated diffraction patterns confirmed the orientation to the 00*L* plane of LDH films (see the Supporting Information). It was observed that the diffraction pattern corresponds to a textured material on the (003) reflection because only one spot appears instead of the typical rings, characteristic of the powder materials. The integrated diffraction pattern is also shown; it is comparative to a Bragg−Brentano diffraction pattern, represented by the MgAl and MgNiAl LDH films. The characteristic 00*L* reflections appeared shifted to lower 2θ angle indicating an expanded interlayer region, as discussed previously.

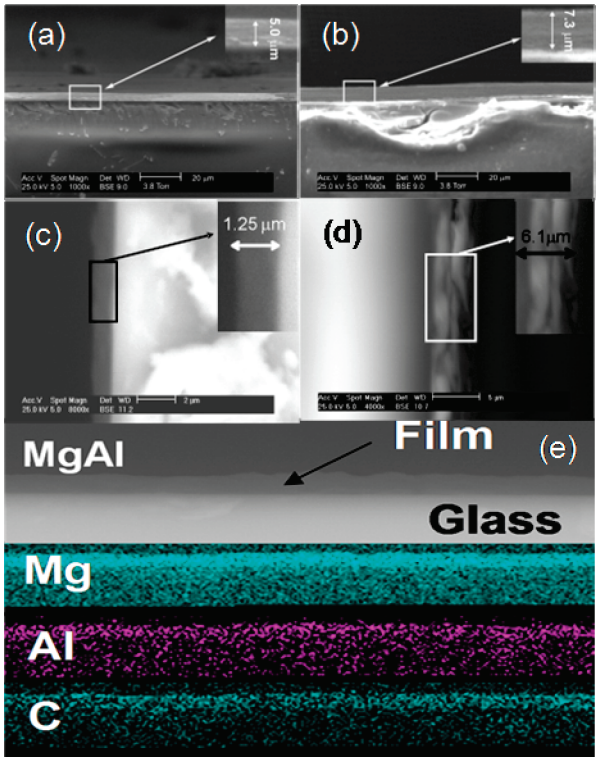

Figure 6. SEM images of thin films: (a) CoNiAl, (b) CoNiAl-2d, (c) NiAl-A, (d) NiAl-A-5d; and (e) SEM image and corresponding elemental map of MgAl film.

Furthermore, the colloidal particle size of sol−gel LDHs results in increased surface-to-surface interactions, which provides an excellent adhesion of the films to polar substrates such as glass.

3.5.1. Scanning Electron Microscopy. SEM images of a variety of thin films over glass substrates are shown in Figure 6. With the aim of controlling film thickness, substrates were immersed in aged sols. As described previously, aging time plays a crucial role in sol−gel synthesis. As the solvent gradually evaporates, condensation and cross-linking reactions accelerate, and the viscosity of the sol increases with time, until it reaches the gelling point.[24,26] Film thickness is directly proportional to sol viscosity. To corroborate this, CoNiAl-2d and NiAl-5d films were prepared by immersing the substrate on 2- and 5-day aged sols, respectively.

CoNiAl (nonaged) film is 5 μm thick and very uniform. After only 2 days aging, viscosity increased enough to increase film thickness ∼150%, to 7.3 μm, as observed in images a and b in Figure 6. The same behavior was observed in NiAl-A samples. Nonaged NiAl-A film (Figure 6c) is 1.25 μm thin. Comparison of images c and d in Figure 6 shows that there is an increase in thickness of nearly 500% from NiAl-A to NiAl-5d. Furthermore, in NiAl-5d, LDH platelets can be observed, with a mean size of ∼10 μm and oriented parallel to the glass substrate, that are formed by condensation and cross-linking reactions and by nanoparticle coalescence and aggregation. These platelets were not observed in the nonaged samples.

3.5.2. Energy-Dispersive X-ray Spectroscopy (EDS). EDS elemental mapping for MgAl LDH film and for

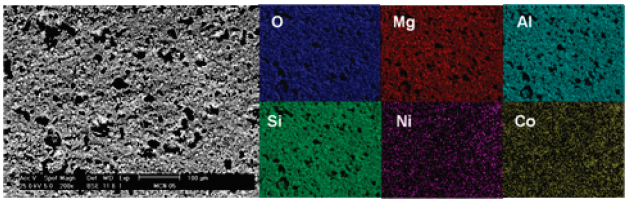

Figure 7. SEM image and corresponding elemental map of calcined CoNiAl catalytic membrane deposited on cordierite monolith.

calcined CoNiAl (i.e., CoNi(Al)O mixed oxide) catalytic membrane were obtained by X-ray mapping technique (SEM/EDS), revealing the elemental distribution in each deposit. The spatial distribution of the emitted energies between the film and the substrate are represented as fading colors; brighter spots indicate higher concentration of the element of interest.

In MgAl LDH film (Figure 6e), EDS reveals a very uniform distribution of magnesium, aluminum, and carbon from the organic interlayer anion. Qualitatively, magnesium has the highest concentration, whereas aluminum and carbon have a lower concentration that appears to be equal among them, in agreement with what is expected on the basis of the stoichiometry of LDHs.

Regarding the catalytic membranes deposited on cordierite monoliths, it was observed by SEM that thickness increased linearly with each immersion (see the Supporting Information). For instance, in CoNi(Al)O, it increased from ca. 5 to 9 to 13 μm with 1, 3, and 5 immersions, respectively. SEM and corresponding EDS of a monolith after 5 immersions in CoNiAl sol is presented in Figure 7. Magnesium and silicon correspond to cordierite; aluminum and oxygen are present both in cordierite and in the deposit; cobalt and nickel are exclusively from the deposit. It can be clearly appreciated that cobalt and nickel are uniformly distributed throughout the surface, and present no agglomeration or sintering despite having been submitted to five calcinations in total. Therefore, it can be concluded that the deposit is very stable and well adhered. These results clearly enable the use of LDHs prepared by this method in a variety of new catalytic applications, such as monolithic reactors and microreactors.

4. Conclusions

A sol−gel method was presented here, which is applicable for the synthesis of LDHs with virtually any chemical composition. The main synthesis parameters were discussed and analyzed based on the fundamental principles of sol−gel science; knowledge of the influence of each of these parameters shall enable the synthesis of sol−gel LDHs with the desired characteristics depending on the intended application. Furthermore, the method may be easily extended to prepare LDHs with compositions different to those presented here. This procedure is a simple way to obtain LDH nanoparticles, which are an intrinsic characteristic of the sol−gel process. The solids obtained by this method show pure LDH structure with low crystallinity and an expanded interlayer region, because of the intercalation of acetate and alkoxy groups, in addition to carbonate and nitrate anions. Textural properties are remarkable, as high surface areas are obtained with a very narrow pore size distribution.

Synthesis of LDHs by the sol−gel method shall enable numerous applications, an example of which is presented here. Thin films with controllable thickness are easily obtained. When sols are deposited on monoliths, followed by calcination, a catalytic membrane is obtained, with a uniform distribution of catalytically active particles and high thermal stability. Furthermore, the mild synthesis conditions throughout the process will permit the direct intercalation of delicate biological and organic molecules.

Acknowledgment. This work was financially supported by the IMP. Technical support from Jaime F. Jaramillo is acknowledged. J.P. thanks Conacyt for a graduate school scholarship.

Supporting Information Available: Details on the reagents and amounts employed for each composition, photographs of transparent gels, N_2 physisorption isotherms and pore size distributions of calcined LDHs, 2D images and corresponding diffraction patterns for LDH thin films, SEM images of CoNiAl impregnated monolith, and main carboxylate binding modes (PDF). This material is available free of charge via the Internet at http://pubs.acs.org.